

# Bionic structure of mechanically coupled diaphragms for sound source localization

QINGSHENG WANG, ZHUSHI RAO, NA TA  
School of Mechanical Engineering  
Shanghai Jiao Tong University  
800 Dongchuan Road, Shanghai, 200240  
P.R.CHINA  
qswang@sjtu.edu.cn

*Abstract:* - The tasks of sound source localization are always of great value in many engineering applications. In these types of localization appliances, several microphone transducers are usually involved in the localization structures. Each of the arrival times of the sound stimulus applied to these microphones is determined individually and sent to the arithmetic-logic sections immediately by which the localization systems could find out positions of the sound sources subsequently. But these appliances always consist of many components, and the looseness of structures may narrow their practical applications. In this paper, a new type of instrument is designed to accomplish the purpose of localizing the sound source by a relatively compact structure. This bionics structure is designed to mimic the localization function of the ears of the parasitoid fly *Ormia ochracea*, and it consists of three elastic diaphragms, three bars which connected to the diaphragms, and the other mechanical components. The analysis of this structure's dynamic behavior shows that the incident angles of the sound have special relationship to the responses of this instrument, and the incident angles can be estimated by detecting the vibrations of the three elastic diaphragms. Compared with traditional microphone arrays, this instrument has the advantage of compaction and higher integrated level.

*Key-Words:* -Vibration and wave, Biomechanics, Bionics, Sound Source localization

## 1 Introduction

Microphone arrays have been used to locate an aerial sound source for many years, these arrays usually consist of 2, 3 microphones or even more [1~3]. The arrival times of the sound stimulus applied to these microphones are determined and sent to the arithmetic-logic sections which could find out position of the sound sources later on. The distance between each two microphones placed in the space is about several centimeters or equivalent amount so that the arrival times of the sound pressures at these microphones can be detected and processed by the subsequent arithmetic-logic sections. The sizes of these appliances are always big relatively, and they usually consist of many components. These physical characters of the structures mentioned above sometimes will limit their applications in industry. And if the microphones, in other words, the acoustic sensory devices, can be placed in very close proximities to each other, these types of sound source localizers will have broader applications definitely. An analysis is presented of mechanical responses to a sound field of the ears of the parasitoid fly *Ormia ochracea* [4~7]. It shows that the ears of this kind of parasitoid fly have a cuticular structure which can couple the ears mechanically in order to achieve the

directional sensitivity. Based on the mechanism of the directional hearing of the parasitoid fly *Ormia ochracea*, some devices were invented as mimic products of the acoustic organ of the parasitoid fly *Ormia ochracea* [8~19].

In this paper, the mechanisms of the parasitoid fly *Ormia ochracea* for sound source localization are discussed. Based upon this, a mini instrument for sound source localization is designed to accomplish the purpose of localizing the sound source by a relatively compact structure. Analysis of the dynamic behavior of this instrument shows that incident angles of the sound have special relationship to the responses of this instrument, and the incident angles can be estimated by detecting the vibrations of it.

## 2 Mechanisms of *Ormia ochracea* for Sound Source Localization

The structure of the ears of the parasitoid fly *Ormia ochracea* and its simplified mechanical model is shown in Fig.1 [4].

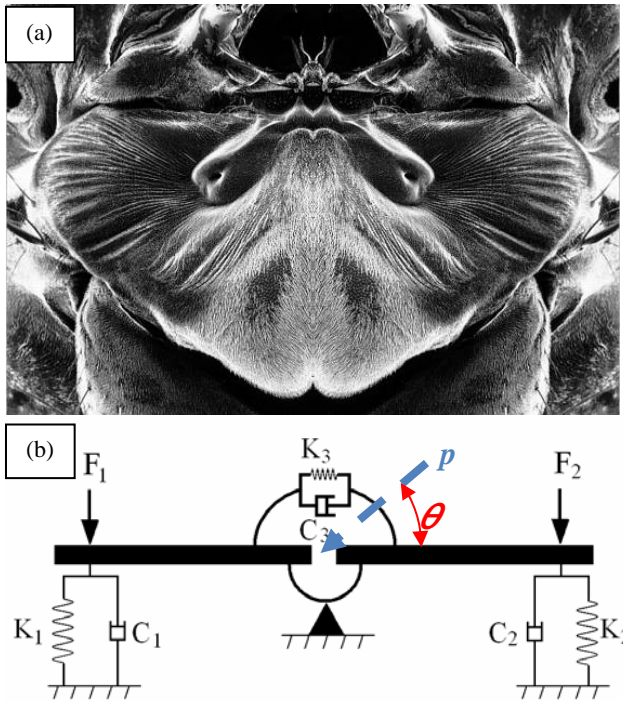


Fig.1 the structure of the hearing organ of the parasitoid fly *Ormia ochracea* and its mechanical model. (a) the prosternal anatomy of the parasitoid fly *Ormia ochracea*. (b) Mechanical modal of the hearing organs of the *Ormia ochracea*.

Let  $x_1$  and  $x_2$  denote the displacement of two ends of the intertympanal bridge shown in Fig.1(b),  $p$  is the incident pressure at the pivot point,  $f_1$  and  $f_2$  the ipsilateral and contralateral forces added up to the two sides of the system by the incident sound stimulus, the transfer functions between the displacement  $x_1$  and  $x_2$  and the incident pressure at the pivot point can be expressed as:

$$H_{x_1p} = \frac{s(k_3 + i\alpha c_3) \times (e^{j\omega\tau/2} - e^{-j\omega\tau/2}) + s(k + i\alpha c - m\omega^2) e^{j\omega\tau/2}}{(k + i\alpha c + k_3 + i\alpha c_3 - m\omega^2)^2 - (k_3 + i\alpha c_3)^2} \quad (1)$$

$$H_{x_2p} = \frac{s(k_3 + i\alpha c_3) \times (e^{-j\omega\tau/2} - e^{j\omega\tau/2}) + s(k + i\alpha c - m\omega^2) e^{-j\omega\tau/2}}{(k + i\alpha c + k_3 + i\alpha c_3 - m\omega^2)^2 - (k_3 + i\alpha c_3)^2} \quad (2)$$

From Eq.(1)(2), let  $H_{x_1x_2}$  denotes the proportion of  $H_{x_1p}$  and  $H_{x_2p}$ , we may obtain Eq.(3):

$$H_{x_1x_2}(\omega) = \frac{H_{x_1p}}{H_{x_2p}} = \frac{L \cdot k_3 + M \cdot c_3 + N_1}{-L \cdot k_3 - M \cdot c_3 + N_2} \quad (3)$$

Where,

$$\begin{aligned} L &= s(e^{i\omega\tau/2} - e^{-i\omega\tau/2}) \\ M &= is\omega(e^{i\omega\tau/2} - e^{-i\omega\tau/2}) \\ N_1 &= s(k + i\omega c - m\omega^2) e^{i\omega\tau/2} \\ N_2 &= s(k + i\omega c - m\omega^2) e^{-i\omega\tau/2} \end{aligned}$$

After selecting the values of the parameters  $k$ ,  $c$ , and  $s$ , and setting the frequency of incident sound

pressure  $f=8\text{kHz}$  which means  $\omega=50240 \text{ rad}\cdot\text{s}^{-1}$  approximately, the incident angle  $\theta=45^\circ$ , the relationship between the magnitude and phase angle of  $H_{x_1x_2}$  and the parameters  $k_3$ ,  $c_3$  can be shown in Fig.2.

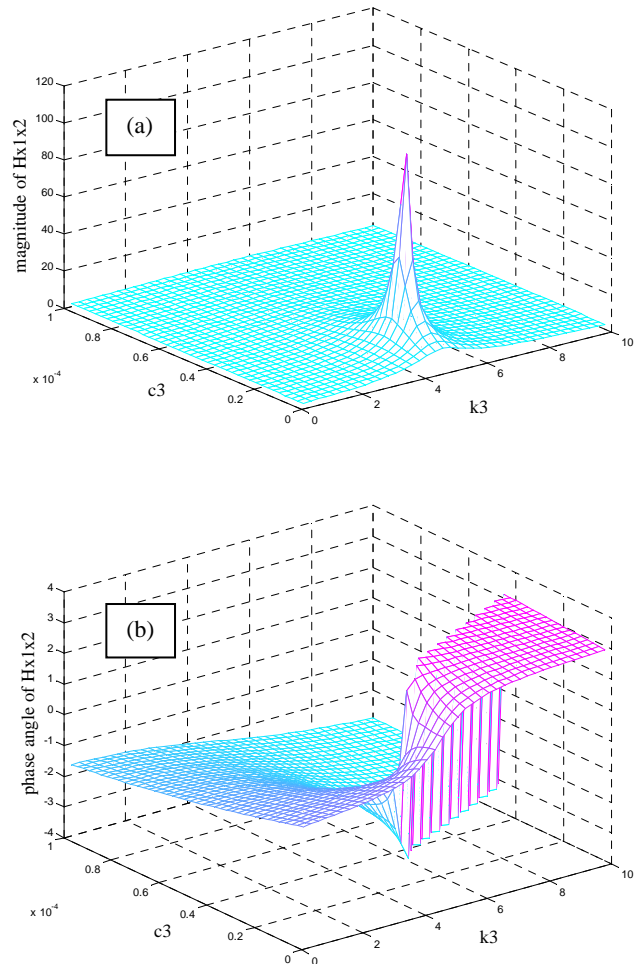


Fig.2 magnitude and phase angle of  $H_{x_1x_2}$  relative to  $k_3$ ,  $c_3$ . (a) magnitude of  $H_{x_1x_2}$ . (b) phase angle of  $H_{x_1x_2}$ .

The general magnitudes of  $H_{x_1x_2}$  are below 20 as the computing result, but there is still an extreme point which may be shown in Fig.2(a). If the point  $(k_3, c_3)$  is near the extreme point, for example,  $k_3=4.67 \text{ N}\cdot\text{m}^{-1}$ ,  $c_3=1.82 \times 10^{-5} \text{ N}\cdot\text{s}\cdot\text{m}^{-1}$ , the magnitude of  $H_{x_1x_2}$  will be considerably large, i.e. the great difference between the responses of the two ends of this model in Fig.3(a) in time domain. Fig.3(b) illustrates time domain response of ipsilateral and contralateral side when  $k_3=5.18 \text{ N}\cdot\text{m}^{-1}$ ,  $c_3=2.88 \times 10^{-5} \text{ N}\cdot\text{s}\cdot\text{m}^{-1}$ . This point is apart from the extreme point, the amplitude of contralateral side response increased compared with Fig.3(a), but still lower than the ipsilateral side significantly.

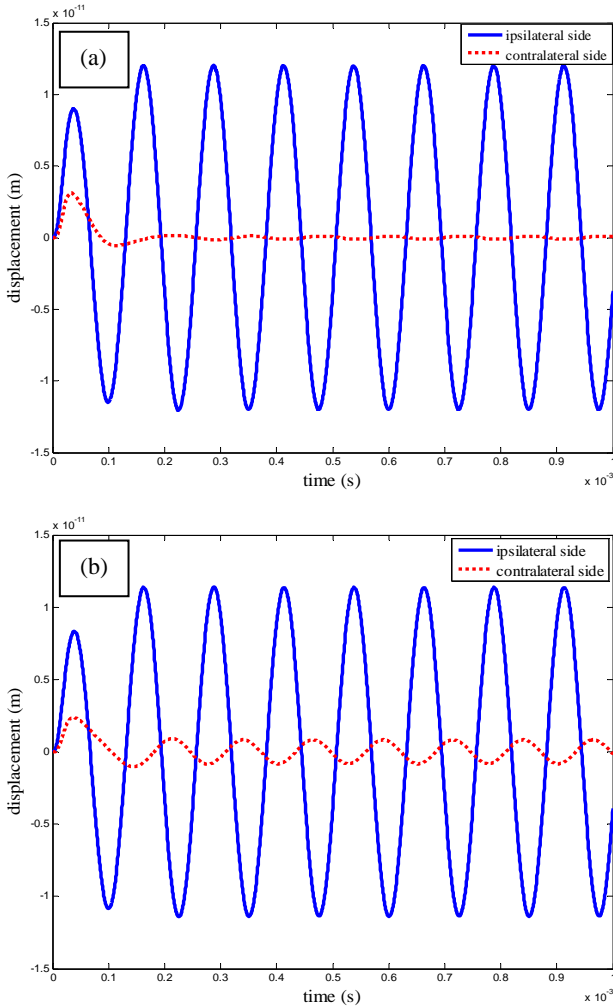


Fig.3 time domain response of ipsilateral and contralateral side. (a)  $k_3=4.67 \text{ N}\cdot\text{m}^{-1}$ ,  $c_3=1.82\times 10^{-5} \text{ N}\cdot\text{s}\cdot\text{m}^{-1}$ . (b)  $k_3=5.18 \text{ N}\cdot\text{m}^{-1}$ ,  $c_3=2.88\times 10^{-5} \text{ N}\cdot\text{s}\cdot\text{m}^{-1}$

After the parameters are given as above (it means the responses of the two ends of this model will be of great difference when the frequency of incident sound is 8kHz), the relationship between the magnitude of  $H_{x_1x_2}$  and the incident angle under various incident frequencies can be shown in Fig.4.

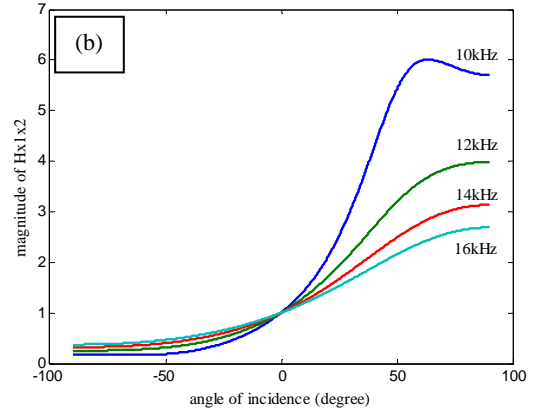
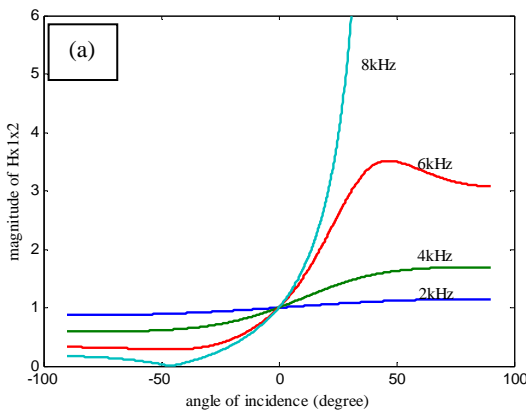


Fig.4 magnitudes of  $H_{x_1x_2}$  relative to incident angles under various incident frequencies form 2kHz to 16kHz. (a) 2kHz to 8kHz. (b) 10kHz to 16kHz

As shown in Fig.4, two localization methods can be supposed as hypothesis to explain how the parasitoid fly localizes the sound source.

The first one is “the relationship between the incident angle and the magnitude of  $H_{x_1x_2}$  should be one-to-one correspondence, and the parasitoid fly *Ormia ochracea* used this mechanism of one-to-one correspondence to accomplish the localization of sound source” (for frequencies from 2kHz to 4kHz, or 12kHz to higher frequencies as shown in Fig.4). The second one is “the parasitoid fly can make use of the sensitivity of this system due to the high grade rate near the point (0,1) in Fig.4 to realize the purpose of finding the sound source when the incident frequency is near the sensitive Frequency ” (especially for the frequencies about 8kHz as shown in Fig.4).

For the first localization approach, the selection of values of  $k_3$ ,  $c_3$  should make sure that  $H_{x_1x_2}$  doesn't have extreme points under the specified sound source's frequency.

Equation (3) can be simplified as:

$$H_{x_1x_2} = \frac{N_1 + N_2}{-L \cdot k_3 - M \cdot c_3 + N_2} - 1 \quad (4)$$

Here,  $\delta$  can be used as an index to make sure that this localization method is available, so,

$$\left| \frac{N_1 + N_2}{-L \cdot k_3 - M \cdot c_3 + N_2} - 1 \right| > \delta$$

Its sufficient condition is:

$$\left| \frac{N_1 + N_2}{-L \cdot k_3 - M \cdot c_3 + N_2} - 1 \right| > \delta$$

i.e.

$$\left( iL \cdot k_3 + \text{Im}(N_2) \right)^2 + \left( M \cdot c_3 - \text{Re}(N_2) \right)^2 < \left( \frac{|N_1 + N_2|}{\delta + 1} \right)^2 \quad (5)$$

This inequation instruction indicates an elliptic region. If the point  $(k_3, c_3)$  is located in this area, the mechanism of one-to-one correspondence will be unavailable, and vice visa. Numerical analysis shows that if the incident frequency is given (in Fig.5(a), it is 8kHz), the trace of this ellipse's center (according to the various incident angle of the sound pressure) is a straight line as shown in Fig.5(b), and the unavailable region of the mechanism of one-to-one correspondence is the area between the two imaginary lines, which is the envelope region of the series of ellipses given by inequation (5). If the mechanism of one-to-one correspondence is desired, the value of  $(k_3, c_3)$  should be out of the unavailable region.

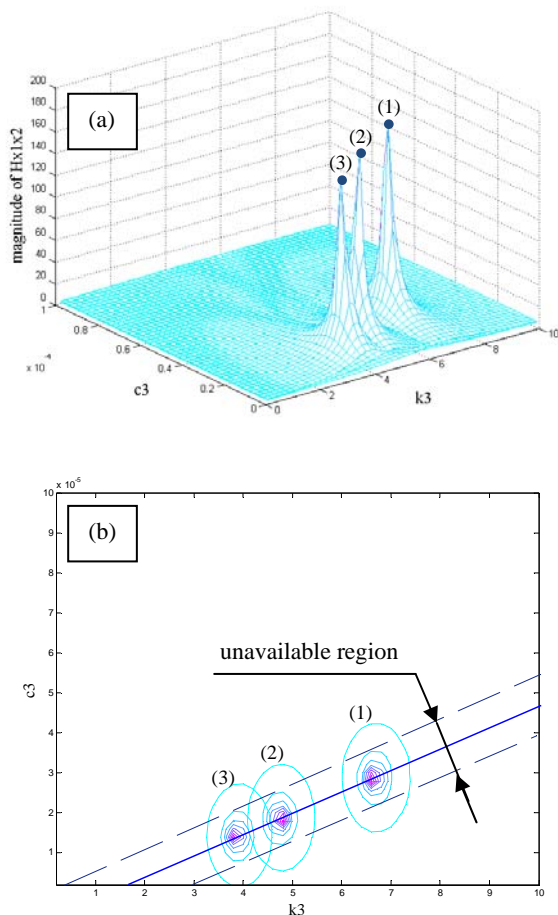


Fig.5 the trace of this ellipse's center and the unavailable region, (1)30°, (2)45°, (3)60°. (a) magnitude of  $H_{x_1x_2}$  when incident angles vary from 30° to 60°. (b) unavailable region by contour map.

For the second localization approach, the procedure to find the incident direction may consist of two separated steps. First, the fly determine the side of the incident sound stimulus to find whether the sound source is in the

ipsilateral or contralateral side, then it may take advantage of the high sensitivity of  $H_{x_1x_2}$  relative to the incident angle when this angle is about zero and under the specified frequencies (For example, 8kHz as shown in Fig.4) due to the high rate of grade. This kind of structure should have a steering hardware so that it can adjust itself in order to direct its normal direction to the sound source.

As mimic bionics structure, the instrument designed for localization may select either one of the two approaches which are mentioned above. In this paper, the first approach is chosen

### 3 structure and features of the sound source localization instrument

In order to locate the sound source in three dimensional space, we will introduce an instrument in this section. The structure of the auditory sensation devices in this instrument is shown in Fig.6.

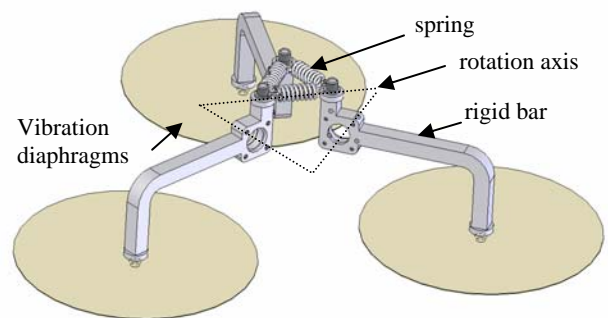


Fig.6 structure of the auditory sensation device in the instrument of sound source localization

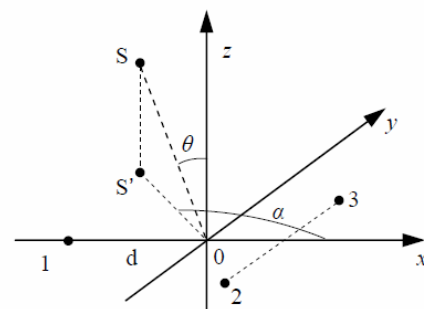


Fig.7 geometrical relationship of the sound source localization

The vibration equation of the structure of the auditory sensation devices described in Fig.8 may be simplified as:

$$\begin{bmatrix} k_1+2k_3 & k_3 & k_3 \\ k_3 & k_1+2k_3 & k_3 \\ k_3 & k_3 & k_1+2k_3 \end{bmatrix} X + \begin{bmatrix} c & 0 & 0 \\ 0 & c & 0 \\ 0 & 0 & c \end{bmatrix} \dot{X} + \begin{bmatrix} m & 0 & 0 \\ 0 & m & 0 \\ 0 & 0 & m \end{bmatrix} \ddot{X} = F \quad (6)$$

The natural frequencies of this system can be shown as:

$$\omega_1 = \omega_2 = \sqrt{\frac{k_1 + k_3}{m}}$$

$$\omega_3 = \sqrt{\frac{k_1 + 4k_3}{m}}$$

and the modes:

$$u_1 = [-1 \quad 1 \quad 0]$$

$$u_2 = [-1 \quad 0 \quad 1]$$

$$u_3 = [1 \quad 1 \quad 1]$$

Let the original point denote the pivot of the structure, and the points labeled 1, 2 and 3 represent the center of the three elastic diaphragms (the three round solid masses). The equation of the plane which normal to the direction of incident sound pressure is:

$$x \sin \theta \cos \alpha + y \sin \theta \sin \alpha + z \cos \theta = 0$$

Suppose  $H_{f_1p}(\omega)$ ,  $H_{f_2p}(\omega)$  and  $H_{f_3p}(\omega)$  are the transfer functions between the forces at the three diaphragms and the incident pressure  $p$  at the pivot point, which can be given by:

$$H_{f_i p}(\omega) = s e^{i\omega\tau_i}$$

Where  $i=1,2,3$  and

$$\tau_1 = \frac{1}{c}(-d \sin \theta \cos \alpha)$$

$$\tau_2 = \frac{1}{2c}(d \sin \theta \cos \alpha - \sqrt{3}d \sin \theta \sin \alpha)$$

$$\tau_3 = \frac{1}{2c}(d \sin \theta \cos \alpha + \sqrt{3}d \sin \theta \sin \alpha)$$

The transfer functions  $H_{x_1p}(\omega)$ ,  $H_{x_2p}(\omega)$  and  $H_{x_3p}(\omega)$  between the displacements  $x_1, x_2, x_3$  at 1, 2, 3 points and the pressure  $p$  at the pivot is

$$\begin{bmatrix} H_{x_1p} \\ H_{x_2p} \\ H_{x_3p} \end{bmatrix} = Z^{-1} \cdot \begin{bmatrix} s e^{i\omega\tau_1} \\ s e^{i\omega\tau_2} \\ s e^{i\omega\tau_3} \end{bmatrix} \quad (7)$$

Where

$$Z = \begin{bmatrix} A & k_3 & k_3 \\ k_3 & A & k_3 \\ k_3 & k_3 & A \end{bmatrix}$$

$$A = -m\omega^2 + j\omega c + k_1 + 2k_3$$

Define  $H_{12}(\omega)$ ,  $H_{23}(\omega)$  and  $H_{31}(\omega)$  as:

$$H_{12}(\omega) = \frac{H_{x_1p}}{H_{x_2p}}$$

$$H_{23}(\omega) = \frac{H_{x_2p}}{H_{x_3p}}$$

$$H_{31}(\omega) = \frac{H_{x_3p}}{H_{x_1p}}$$

From Eq.(6)(7), we introduce the mechanism of one-to-one correspondence for sound source localization as follows:

$$\sin \theta = \sqrt{D_1^2 + D_2^2}$$

$$\sin \alpha = \frac{D_1}{\sqrt{D_1^2 + D_2^2}} \quad (8)$$

$$\cos \alpha = \frac{D_2}{\sqrt{D_1^2 + D_2^2}}$$

Where:

$$D_1 = \frac{cc}{j\sqrt{3}\omega d} \cdot \ln \frac{k_3 H_{13} + k_3 H_{23} + A}{k_3 H_{13} + A H_{23} + k_3}$$

$$D_2 = \frac{cc}{j3\omega d} \cdot \left[ \ln \frac{k_3 H_{13} + A H_{23} + k_3}{A H_{13} + k_3 H_{23} + k_3} + \ln \frac{k_3 H_{13} + k_3 H_{23} + A}{A H_{13} + k_3 H_{23} + k_3} \right]$$

This localization method is available when

$$f \leq \frac{cc}{4d}$$

### 4 Experiment

According to the localization mechanism mentioned above, a sound source localization instrument used mechanically coupled diaphragms is designed as shown in Fig.8.

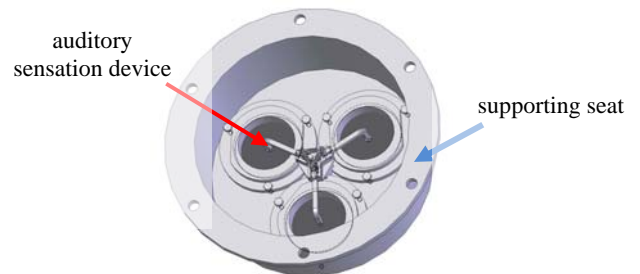


Fig.8 the structure diagram of the sound source localization instrument

To eliminate interference of the ambient noise, this localization instrument is placed in a polymethyl methacrylate case, and the front face of it is exposed

outside across the pore on the side board. The three laser sensor are used to detect the vibrations of the three diaphragms. The disposal of the localization instrument and the laser displacement sensor is illustrated as Fig.9, and the general structure of the test system is as Fig.10.

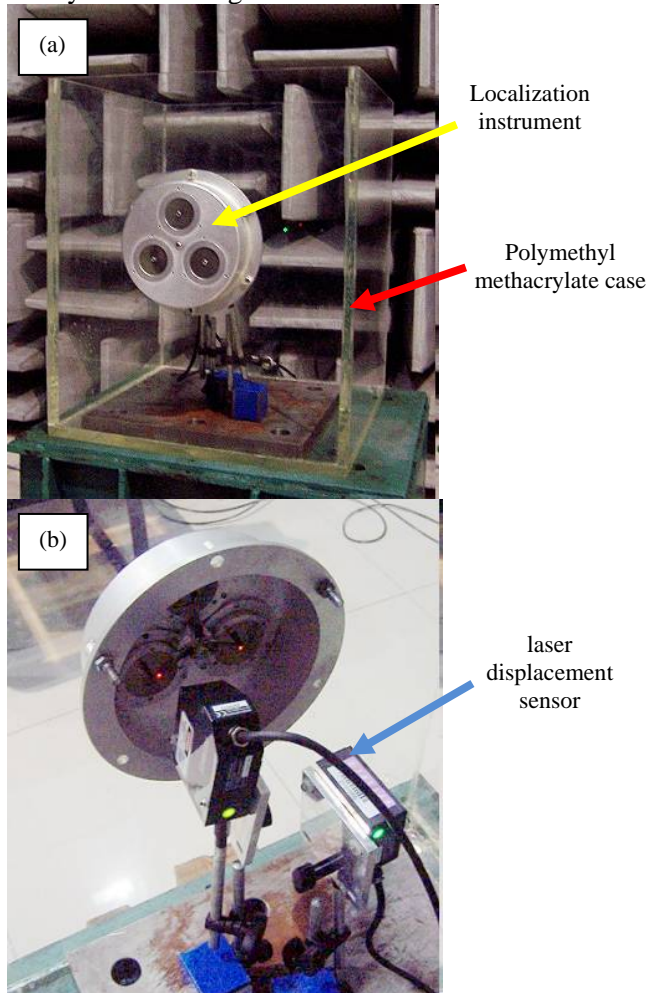


Fig.9 disposal of the localization instrument and the laser displacement sensor. (a) the localization instrument on the side board. (b) the laser displacement sensors placed inside the polymethyl methacrylate case.

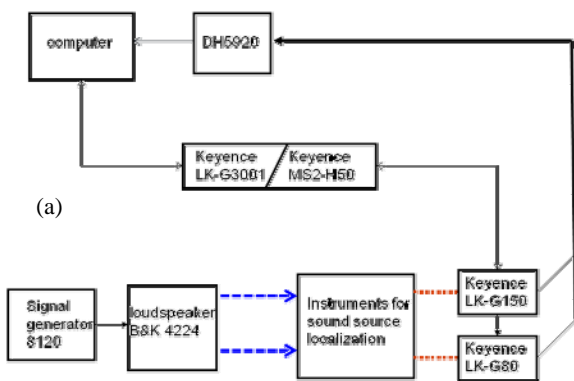


Fig.10 (a)general structure of the test system. Blue arrows indicate the sound stimulus generated by the

loudspeaker B&K 4224 and the signal generator 8120. Red imaginal lines indicate the laser for test.

Data of diaphragms vibration displacement are collected by data acquisition instrument DH5920 and sent to computer for analyzing. (b) data acquisition instrument DH5920. (c) signal generator 8120. (d) loudspeaker B&K 4224. (e) signal and power supply adapter.

Fig.11 and Fig.12 illustrate the time domain response and spectrum of the three measure points displacements when the angle  $(\theta, \alpha)=(45^\circ, 270^\circ)$ .

Making some alternation to the incident angle as  $(30^\circ, 87^\circ)$ ,  $(30^\circ, 84^\circ)$ ,  $(30^\circ, 81^\circ)$ ,  $(30^\circ, 78^\circ)$ , the vibrations of the three diaphragms can be obtained via the measurement system.

The time domain response of the three vibration diaphragms and displacement spectrums can be shown in Fig.13~Fig.20, and the calculated values of incident angle can be obtained according to Eq.(8), as shown in Table.2, which could be compared with the actual values in Fig.21.

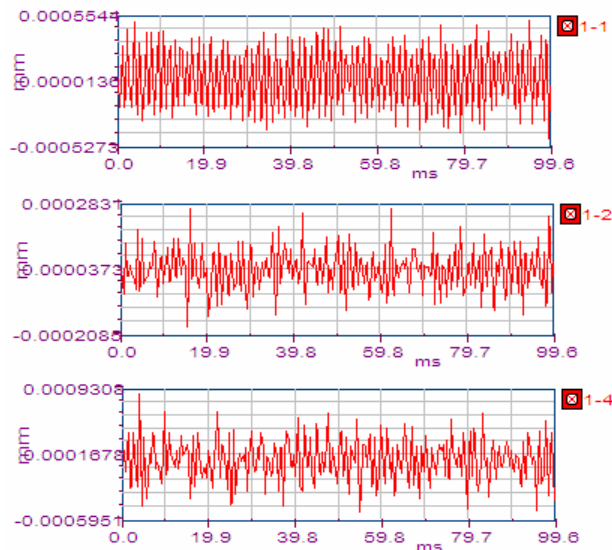


Fig.11 time domain response of the three measure points when the incident angle  $(\theta, \alpha)= (45^\circ, 270^\circ)$

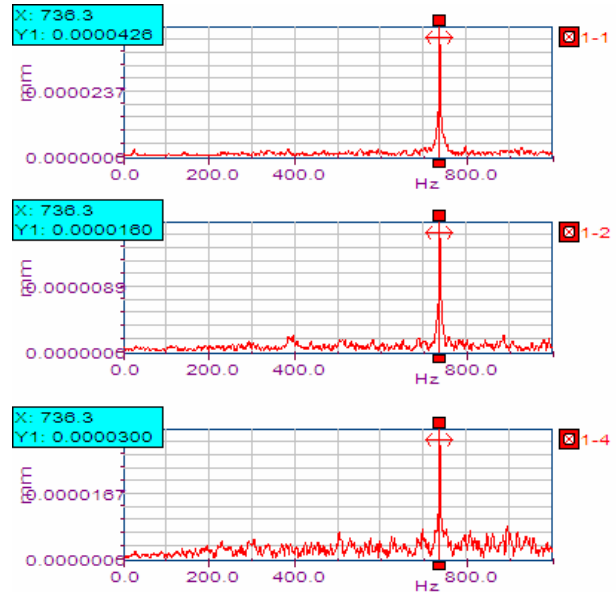


Fig.12 displacement spectrums of the three measure points when the incident angle  $(\theta, \alpha)=(45^\circ, 270^\circ)$  Parameters of this model are given by Table.1.

Table.1 parameters of the mechanical model of the localization instrument

| parameters | values                               |
|------------|--------------------------------------|
| $m$        | $4.81011 \times 10^{-3} \text{kg}$   |
| $c$        | $2.2 \times 10^{-6} \text{Nsm}^{-1}$ |
| $k_1$      | $1.5218 \times 10^4 \text{Nm}^{-1}$  |
| $k_3$      | $1.2012 \times 10^3 \text{Nm}^{-1}$  |
| $c$        | $340 \text{ms}^{-2}$                 |
| $\omega$   | $740 \text{Hz}$                      |
| $d$        | $0.050 \text{m}$                     |

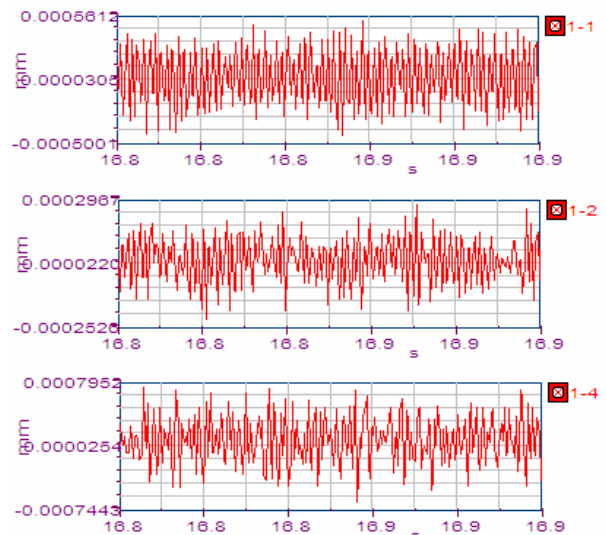


Fig.13 time domain response of the three measure points when the incident angle  $(\theta, \alpha)= (30^\circ, 87^\circ)$

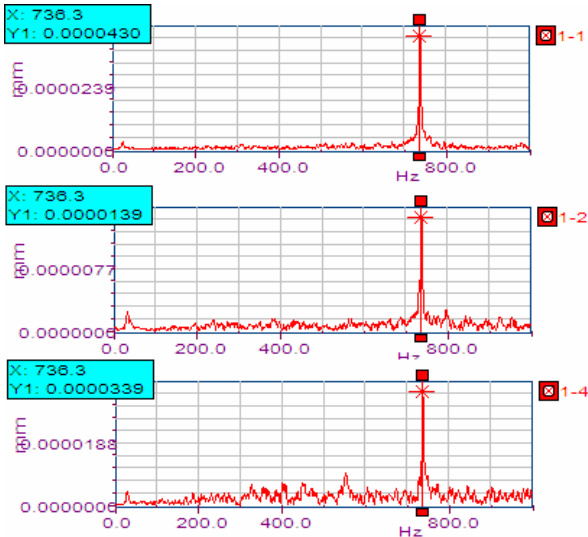


Fig.14 displacement spectrums of the three measure points when the incident angle  $(\theta, \alpha)=(30^\circ, 87^\circ)$

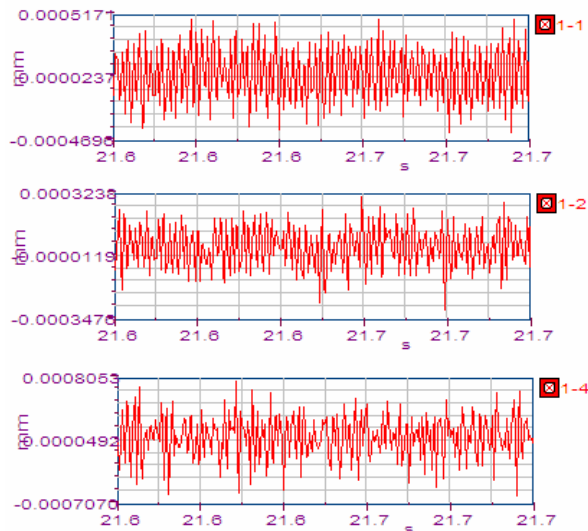


Fig.15 time domain response of the three measure points when the incident angle  $(\theta, \alpha)=(30^\circ, 84^\circ)$

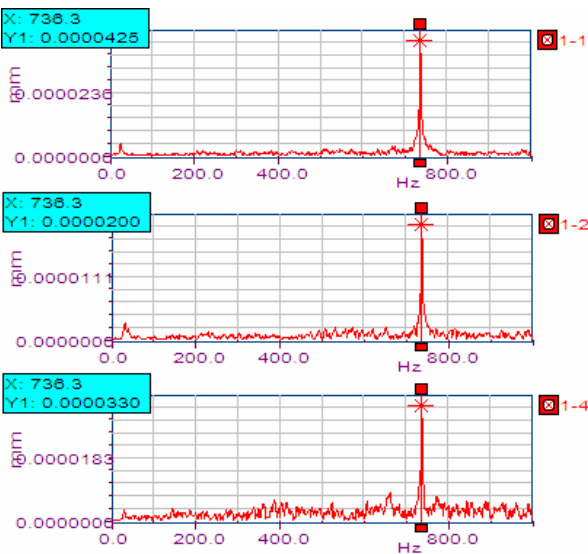


Fig.16 displacement spectrums of the three measure points when the incident angle  $(\theta, \alpha)=(30^\circ, 84^\circ)$

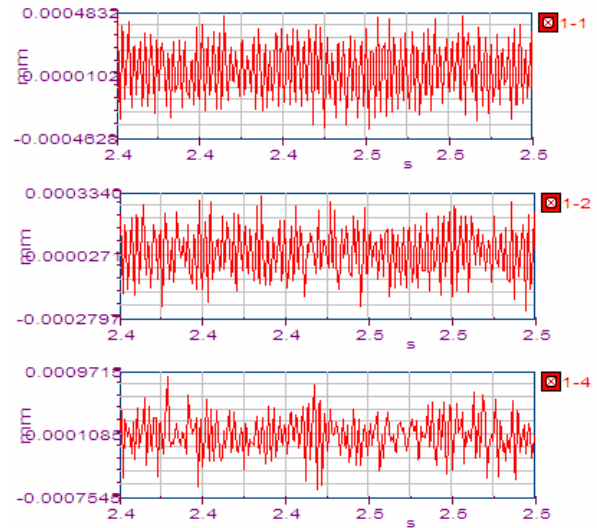


Fig.17 time domain response of the three measure points when the incident angle  $(\theta, \alpha)=(30^\circ, 81^\circ)$

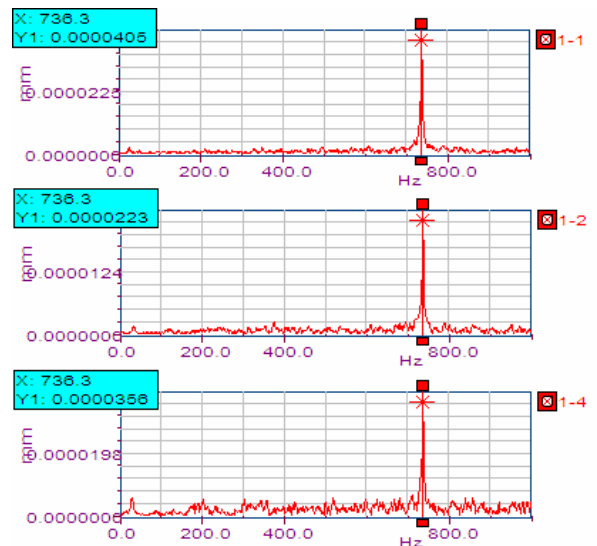


Fig.18 displacement spectrums of the three measure points when the incident angle  $(\theta, \alpha)=(30^\circ, 81^\circ)$

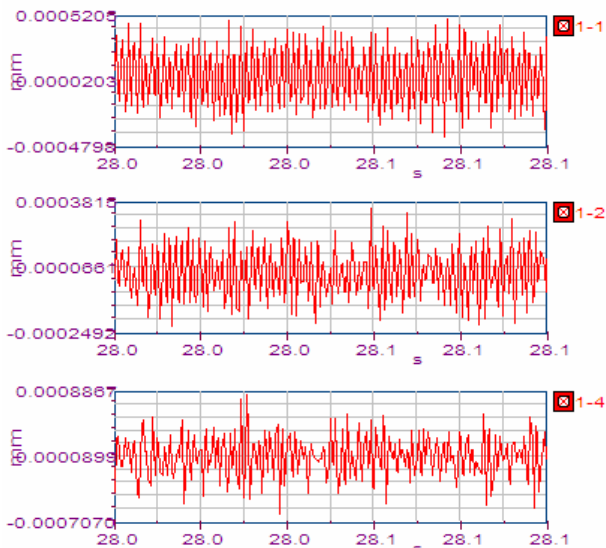


Fig.19 time domain response of the three measure points when the incident angle  $(\theta, \alpha) = (30^\circ, 78^\circ)$

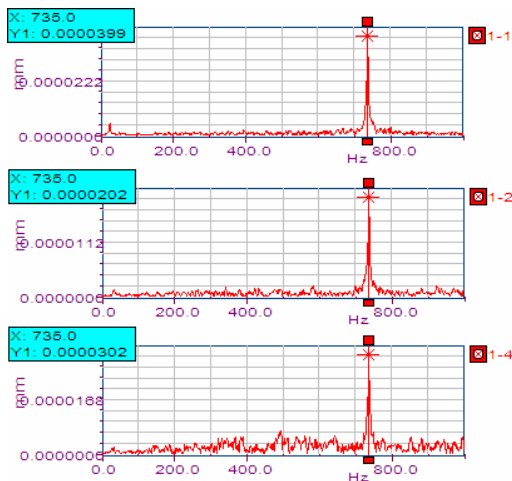


Fig.20 time domain response of the three measure points when the incident angle  $(\theta, \alpha) = (30^\circ, 78^\circ)$

Table.2 comparison of the actual value and calculated value of  $(\theta, \alpha)$

| actual value           | calculated value             | maximal error |
|------------------------|------------------------------|---------------|
| $(30^\circ, 87^\circ)$ | $(26.74^\circ, 91.41^\circ)$ | 4.41°         |
| $(30^\circ, 84^\circ)$ | $(27.63^\circ, 85.52^\circ)$ | 2.37°         |
| $(30^\circ, 81^\circ)$ | $(26.55^\circ, 83.72^\circ)$ | 3.45°         |
| $(30^\circ, 78^\circ)$ | $(24.74^\circ, 80.83^\circ)$ | 5.26°         |

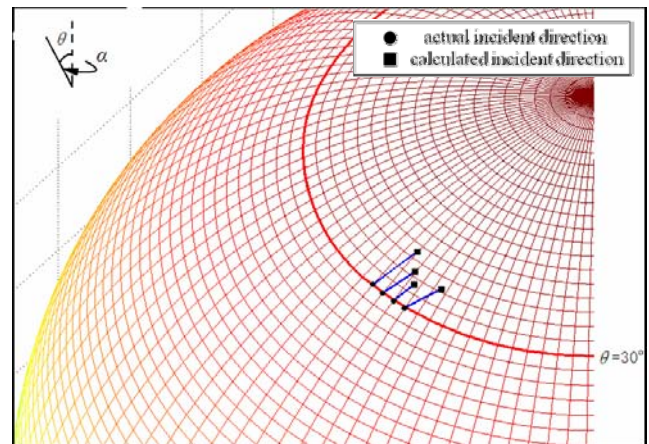


Fig.21 comparison of the actual incident direction and calculated direction

### 5 Conclusion

The mechanisms of the parasitoid fly *Ormia ochracea* for sound source localization are discussed and two kinds of approaches for sound source localization are introduced in section.1 of this paper. Based upon this, a mini instrument for sound source localization is designed to accomplish the purpose of localizing the sound source by a relatively compact structure.

The analysis of the dynamic behavior of this instrument shows that the incident angle of the sound has special relationship to the respond of this instrument, and the incident angle can be estimated by detecting the vibrations of it, these may owe to the localization approach of one-to-one correspondence of the incident angles  $(\theta, \alpha)$  and the values of  $(H_{12}, H_{23}, H_{31})$ .

The experimental results reveal that the localization instrument has certain accuracy and verified the localization mechanism finely.

### References:

- [1] Futoshi Asano, Hideki Asoh, Toshihiro Matsui, Sound Source Localization and Separation in Near Field. *IEICE TRANSACTIONS on Fundamentals of Electronics, Communications and Computer, Sciences*, Vol.E83-A No.11, pp. 2286-2294
- [2] Tsuji.T, Yamamoto.K, Ishii.I, Real-time Sound Source Localization Based on Audiovisual Frequency Integration. *Pattern Recognition, 2006. ICPR 2006. 18th International Conference*, Vol.4, pp.322 – 325
- [3] Jie Huang, Ohnishi N, Sugie N, A Biomimetic System for Localization and Separation of Multiple Sound Sources. *Instrumentation and Measurement, IEEE Transactions*, 1995; 44 (3)

- [4] Miles, R.N, Robert, D, Hoy, R.R, Mechanically coupled ears for directional hearing in the parasitoid fly *Ormia ochracea*. *Journal of the Acoustical Society of America*, v 98, n 6, Dec, 1995, pp.3059-3070
- [5] D.Robert, R.N.Miles, R.R.Hoy, Tympanal mechanics in the parasitoid fly *Ormia ochracea*: intertympanal coupling during mechanical vibration. *J comp Physiol A* (1998) 183, pp.443-452.
- [6] Daniel Robert, Urban Willi. The histological architecture of the auditory organs in the parasitoid fly *Ormia ochracea*. *Cell Tissue Res* (2000)301, pp.447-457
- [7] Akcakaya, Murat; Nehorai, Arye. Performance analysis of the *Ormia ochracea*'s coupled ears, *Journal of the Acoustical Society of America*, 2008, v 124, n 4, pp.2100-2105,
- [8] Tadigotla.Viswanath, Commuri.S, Design and implementation of Reconfigurable Mobile Sensor Systems, *WSEAS Transactions on Systems*, v 6, n 2, pp.400-408, February 2007
- [9] Pollastrone. Fabio, Neri.Carlo, System for semi-automatic optical radar probe alignment, *WSEAS Transactions on Systems*, v 4, n 11, pp.1946-1951, November 2005
- [10] Velasco-Herrera, Graciela, Parallel micro-manipulator system with applications in micro assembles and micro machine-making, *WSEAS Transactions on Systems*, v 4, n 7, pp.980-987, July 2005
- [11] Miles.R.N, Su. Q, Cui.W, Shetye. M, Degertekin.F.L, Bicen.B, Garcia.C, Jones.S, Hall. N, A low-noise differential microphone inspired by the ears of the parasitoid fly *Ormia ochracea*. *Journal of the Acoustical Society of America*. 2009, v 125, n 4, pp.2013-2026,
- [12] Miles R.N, Novel Biologically-inspired directional microphones. *Echo*, 2007; 17(2)
- [13] CUI Weili, Bicen B, Hall N, Jones S.A, Degertekin F.L, Miles R.N, Optical sensing in a directional MEMS microphone inspired by the ears of the parasitoid fly, *Ormia ochracea*, IEEE, *MEMS2006, Istanbul, Turkey*, 2006, pp.22-26
- [14] Saito A, Ono N, Ando S, Micro gimbals diaphragm for sound source localization with mimicking *Ormia Ochracea*, *Proceedings of the 41st SICE Annual Conference*, Aug.5-7, 2002, Osaka, pp.1640-1643.
- [15] K. Yoo, C. Gibbons, Q. T. Su, R. N. Miles, N. C. Tien, Fabrication of biomimetic 3-D structured diaphragms, *Sensors and Actuators A: Physical*, Vol.97-98, 1 April 2002, pp.448-456
- [16] Oshinsky ML, Hoy R.R, Physiology of the auditory afferents in an acoustic parasitoid fly [J]. *The journal of Neuroscience*, 2002, 22(16), pp.7254-7263
- [17] C.Gibbons. Design of a biomimetic directional microphone diaphragm, *Masters Thesis, Binghamton University*, 2000
- [18] Homentcovschi. Dorel, Aubrey.Matthew.J, Miles, Ronald N, A two-dimensional model of a directional microphone: Calculation of the normal force and moment on the diaphragm. *Journal of the Acoustical Society of America*. February 2006, v 119, n 2, pp.756-768,
- [19] Cui. Weili, Bicen. Baris, Hall. Neal, Jones. Stephen A, Degertekin. F. Levent, Miles. Ronald N, Optical sensing in a directional MEMS microphone inspired by the ears of the parasitoid fly, *Ormia Ochracea*. *Proceedings of the IEEE International Conference on Micro Electro Mechanical Systems (MEMS)*, v 2006, pp614-617, 2006,
- [20] Chen. L, Dong. Yue-Hang, Yin. Cheng-Liang, Zhang. Jian-Wu, System dynamic modeling and optimal torque control strategy for E.T. driver based on AMT. *WSEAS Transactions on Systems*, v 7, n 7, pp.742-757, July 2008
- [21] Maidi. Ahmed, Diaf. M, Khelassi. A, Bouyahiaoui. C, Non-interacting fuzzy control system design for distillation columns. *WSEAS Transactions on Circuits and Systems*, v 4, n 4, pp.345-350, April 2005
- [22] Srivastava. Smriti, Bansal. Ankur, Chopra. Deepak, Goel. Gaurav, Modeling and control of a Choquet Fuzzy Integral based controller on a real time system. *WSEAS Transactions on Systems*, v 5, n 7, pp.1571-1578, July 2006
- [23] Amlani, A. M, Rakerd. B, Punch. J. L, Speech clarity judgments of hearing-aid-processed speech in noise: Differing polar patterns and acoustic environments, *Int. J. Audiol.* 45, pp.319-330.
- [24] Ando. S, Ono. N, Fujita. Y, Partial differential equation-based algorithm of sound source localization with finest granularity in both time and frequency, *Proceedings of International Conference Networked Sensing Systems (INSS2007)*, pp. 229-234.
- [25] Stanacevic. M, Cauwenberghs. G, Micropower gradient flow acoustic localizer, *IEEE Trans. Circuits Syst., I: Regul. Pap.* 52, pp.2148-2157.
- [26] Miles. R. N, Cui. W, Miller. R. A, Su. Q, Tan. L, Weinstein. M. G, Response of a biologically inspired MEMS differential microphone diaphragm, *Proceedings of the SPIE AeroSense 2000, Orlando, FL*, pp. 4743-15.

- [27] Hall. N. A, Bicen. B, Lee. W, Jeelani. K, Qureshi. S, Okandan. M, Degertekin. F. L, Micromachined microphones with diffraction-based optical displacement detection, *J. Acoust. Soc. Am.* 118, pp.3000–3009.
- [28] Hall. N. A, Degertekin. F. L, An integrated optical interferometric detection method for micromachined capacitive acoustic transducers, *Appl. Phys. Lett.* 80, pp.3859–3861.
- [29] Tavakolpour. A.R, Mat Darus. I.Z, Mailah. M, Numerical simulation of a flexible plate system for vibration control. *WSEAS Transactions on Systems and Control*, v 4, n 3, pp.119-128, March 2009.
- [30] Al-Gawagzeh, Mohammed Yousef , Al-Hadidi, Mohammed Rasoul, Effect of strong linear polarization anisotropy on geometrical modes characteristics of optical fiber. *WSEAS Transactions on Communications*, v 8, n 1, pp.1-10, 2009
- [31] Qaqish. Maher Akawwi. Emad, Fadda, Eyad, Comparison between computed shearing forces by AASHTO specifications and finite element method of two continuous spans of voided slab bridge. *WSEAS Transactions on Information Science and Applications*, v 6, n 4, pp.621-636, 2009
- [32] Dinis, Corina Maria, Popa, Gabriel Nicolae, Iagar Angela, Mathematical modeling and simulation in Matlab/Simulink of processes from iron ore sintering plants. *WSEAS Transactions on Systems*, v 8, n 1, pp.34-43, 2009
- [33] Cheng Yao-Yu, Li Yong-Hong, Hu Yan, Liu Yan-Hua, The analysis and correction of factors influencing imaging quality of digital radiographic testing system. *WSEAS Transactions on Mathematics*, v 7, n 5, pp.283-292, May 2008
- [34] Arthur. Ben J, Hoy. Ronald R, The ability of the parasitoid fly *Ormia ochracea* to distinguish sounds in the vertical plane. *Journal of the Acoustical Society of America*, v 120, n 3, pp.1546-1549, 2006